Organogels from Different Self-Assembling New Dendritic Peptides: Morphology, Reheology, and Structural Investigations

ARTICLE *in* THE JOURNAL OF PHYSICAL CHEMISTRY B · JANUARY 2010

Impact Factor: 3.3 · DOI: 10.1021/jp908011v · Source: PubMed

Organogels from Different Self-Assembling New Dendritic Peptides: Morphology, Reheology, and Structural Investigations

Goutam Palui,[†] Ashesh Garai,[‡] Jayanta Nanda,[†] Arun Kumar Nandi,*[,‡] and Arindam Banerjee*[,†]

Department of Biological Chemistry and Polymer Science Unit, Indian Association for the Cultivation of Science, Jadavpur, Kolkata 700 032, India

Received: August 19, 2009; Revised Manuscript Received: December 2, 2009

Three new peptide based dendrimers with different generations were synthesized, purified, and characterized. Each of these dendrimers form efficient organogels under suitable conditions and these gels were characterized by field emission scanning electron microscopy (FE-SEM), high resolution transmission electron microscopy (HR-TEM), atomic force microscopy (AFM), Fourier transformed infrared (FT-IR) spectroscopy, differential scanning calorimetery (DSC) and rheology. It has been observed that gel forming propensity increases from first to second generation dendrimer and it decreases from second to third generation. The hydrogen bonding interaction is the main driving force for the formation of aggregated structure that leads to the formation of a fibrillar network, responsible for gelation. The morphology is network type consisting of taped or twisted fibrils spanning throughout the space. DSC measurements show the thermorevsible first-order phase transition. Rheological studies indicate that flow behavior and segmental motion of these gels are different for different peptidic gels, obtained from various generations of dendritic peptides.

Introduction

Low molecular weight gels obtained from various self-assembling small organic molecules have received significant attention due to their various applications including structure directing agents,[1] stabilization of organic photochromatic material,[2] in situ formation and stabilization of nanoparticles,[3] light harvesting materials,[4] drug delivery systems,[5] dental composite carriers,[6] preparing dye sensitized solar cells,[7] and others.[8] So, the preparations of gel forming systems[9] are of increasing interest for the discovery of new soft materials having some interesting properties. In recent years, several groups like Hanabusa et al.,[9g,10a,b] Bhattacharya et al.,[10c−f] Suzuki et al.,[9g,10a,b] and Fages et al.[10g−i] made significant contributions on the design and synthesis of thermoreversible, low molecular weight gelators based on amino acids.[10] Novel fluorescent organogels containing a chromophoric moiety can be used as light harvesting materials[4,11] and for other purposes.[12] In a recent report, Bhattacharya et al. has demonstrated that there are some controlling factors for the formation of photochromic organogels using various low molecular weight organic molecules.[13] However, dendritic gelators are not so extensively studied, as these gelators are relatively difficult to make and purify. Dendritic gels can create a bridge between polymeric and low molecular weight (LMW) gels. These dendritic gelators can be considered as intermediate between polymeric and LMW gels in terms of molecular weight. Moreover, they possess a well-defined and readily controllable structure that is a prerequisite condition for the construction of a functional gel phase material. These dendritic gels have started getting some attention for last several years,[14] and they exhibit thermoreversibility like low molecular mass gels. In the early 1990s, Newkome and co-workers[15] reported the initial work on dendritic hydrogels based on dendritic bola-amphiphiles having hydrophilic surfaces and hydrophobic interiors. Their pioneering work has led to the discovery of various dendritic gelators. Simanek and co-workers[16] reported dendritic gels based on triazines, and they showed that gelation property depends on the selection of linking and surface groups present in those dendritic gelators. Grinstaff et al.[17] reported the synthesis of dendritic-linear hybrid polymers containing methyl acryl units on the periphery. In addition, Stupp and co-workers[18] developed a series of rod−coil hybrid dendritic organogelators with a potential application in electronic devices. However, there is relatively less work reported on the self-assembly of natural amino acid based dendrimers that can form gels under suitable conditions.[19,14e] Particularly, the dendritic gelators based on amino acids are of much interest because they are constituted from proteinogenic amino acid building blocks and they are expected to be biocompatible. Previously Smith et al.[20] reported the systematic study of the dendritic gelators based on L-lysine. They described on the effect of the different leading factors such as spacer chain, generation of dendrons and dendrimers, solvents, stereochemistry, stoichiometric ratio of the two components, and peripheral groups on the gelation. Kim and co-workers[21] have also used amide dendrons for the construction of gel phase materials. They form gels at relatively higher concentrations, showing the negative dendritic effect in their gel formation. In a recent report, it has been described that self-assembling amino acid based dendrons form organogels in various organic solvents, and these gels exhibit lyotropic and thermotopic liquid crystalline behavior.[22] Photoreversible dendritic organogels have been obtained from the second-generation poly(Gly-Asp) dendrons containing an azobenzene focal point.[23] Chow et al. studied self-assembly and gelation of α-amino acid based synthetic new dendrons, and these dendritic molecules also exhibit sequence-dependent organogelation property.[24] In a very recent report by Chen et al., it has been demonstrated

* Corresponding author. Fax: +91-332473-2805. Tel: +91-332473-4971. E-mail: bcab@iacs.res.in and arindam.bolpur@yahoo.co.in; Fax: +91-332473-2805; Tel: +91-332473-4971; E-mail: psuakn@iacs.res.in.
[†] Department of Biological Chemistry.
[‡] Polymer Science Unit.

10.1021/jp908011v
Published on Web 12/31/2009

that supramolecular organogels are formed from self-assembling dumble shaped dendritic molecules containing *p*-terphenylene moiety as core and these gels exhibit strong fluorescent emission, which is induced by self-aggregation.[25] They showed the negative dendritic effect and this is due to the increase of sterically hindered peripheral alkyl groups.

Our research group has been engaged in studying self-assembly and gelation of synthetic linear oligopetides[26] and dendritic peptides.[27] In the previous work, we have discussed the thermodynamic parameters and morphological changes of different dendrimeric gels having only one generation in different solvents.[27] However, in the course of our investigations with the various self-assembling dendritic peptides, it was observed that three different generations of dendritic peptides (Figure 1) form organogels in various organic solvents including tetralene, 1,2-dichlorobenzene, chlorobenzene, *o*-, *m*-, *p*-xylene, and nitrobenzene at a low concentration (Table 1). These gels are characterized using various techniques including TEM, FE-SEM, AFM, FT-IR, DSC, and rheological properties of these gels are also thoroughly investigated. The morphology of the gel material changes with respect to the change of generation of the dendrimeric gelator keeping the solvent system constant. It is interesting to address the question whether rheological property can vary from one generation to another and it is remarkable to note that rheological properties like flow behavior and segmental motion of these dendritic peptide based gels vary from one generation to the other.

Experimental Section

General Methods and Materials. Fumaric acid, HOBt (1-hydroxybenzotriazole), DCC (1,3-dicyclohexylcarbodiimide), and amino acids were purchased from Sigma chemicals.

Synthesis. The dendrimers based on L-aspartic acid (Figure 1) were synthesized in optically pure form using a convergent coupling methodology. A solution-phase approach was used to get the desired compounds. DCC (1,3-dicyclohexylcarbodiimide) was used as coupling agent and HOBt (1-hydroxybenzotriazole) was used to suppress the racemization of the chiral centers. The final products were purified by column chromatography using silica (100−200 mesh size) gel as the stationary phase and chloroform:methanol (95:5) mixture as the eluent, and the products were characterized using ^{1}H NMR, ^{13}C NMR, and ESI-MS techniques. The synthetic procedure has been given in detail in the Supporting Information.

NMR Experiments. All NMR studies were carried out on a Brüker DPX 300 MHz spectrometer at 300 K. Compound concentrations were in the range 1−10 mmol in $CDCl_3$ or DMSO-d_6.

Mass Spectrometry. Mass spectra were recorded on a Q-Tof micro™ (Waters Corp.) mass spectrometer by positive mode electrospray ionization.

FT-IR Spectroscopy. FT-IR spectroscopy was performed using Nicolate 380 FT-IR spectrophotometer (Thermo Scientific). All reported FT-IR spectra were taken using the spectroscopic cell with a NaCl window in the case of a dilute solution of gelators and with the KBr pellet technique for measurements of wet gels. During the recording of IR spectra using the NaCl cell for the diluted solution of dendritic gelators, 100 scans were performed and the solvent (1,2-dichlorobenzene) subtraction technique was performed.

Field Emission Scanning Electron Microscopic Study. Morphologies of all reported gel materials were investigated using field emission scanning electron microscopy (FE-SEM). For SEM study, the dilute solution of gel materials was dried and platinum coating was carried out. Then the micrographs were taken in a SEM apparatus (JEOL Scanning Microscope-JSM-6700F).

Transmission Electron Microscopic Study. Morphologies of the reported gels were investigated using a transmission electron microscope (TEM). Transmission electron microscopic study was done by placing a drop of a very dilute solution of gel phase material of the corresponding compounds on carbon-coated copper grids (300 mesh). The grid was then allowed to dry in vacuum at 30 °C for 2 days. Images were taken by an FEI (Tecnai spirit) instrument.

Atomic Force Microscopic Study. Morphologies of the reported organogels were investigated using atomic force microscope (AFM). AFM studies were done by placing a small amount of gel (at its minimum gelation concentration) of the corresponding compounds on a microscopic cover glass and then dried by slow evaporation. The material was then allowed to dry in vacuum at 30 °C for 2 days. Images were taken by an AUTOPROBE CP base unit, di CP-II instrument, model no. AP-0100.

Differential Scanning Calorimetry. To find out the T_g, melting temperature, and other thermal behavior, a Perkin-Elmer differential scanning calorimeter (Diamond DSC-7) working under a N_2 atmosphere was used. Gel samples were taken in large volume capsules (LVC) tightly sealed with an O-ring. These samples were then heated from 0 to 160 °C at the heating rate of 10 °C/min. Cooling runs were also taken after waiting 10 min at 160 °C and then cooled at the rate 5 °C/min to 0 °C. Samples were heated again from 0 to 160 °C. The instrument was calibrated with indium and cyclohexane.

Rheological Measurements. Rheological experiments were done using an Advanced Rheometer AR 2000 (TA Instruments) by cone and plate geometry in a peltier plate. The cone diameter was 40 mm, cone angle 1° 59′ 50″, and truncation 56 μm. Two types of experiments were performed: (i) by changing shear rate (at 30 °C) and (ii) by temperature ramp (from 30 to 170 °C) methods. Because of rapid evaporation of *o*-dichlorobenzene the experiments were not performed above 170 °C.

Results and Discussion

Peptide based gelators are a somewhat different kind of gelators than those based on fatty acylated amino acid systems. This is because the former class of gelators has more H-bonding sites available than that of the latter class of amino acid based gelators in which H-bonding can only participate through interamide association.[28] So, the presence of multiple amide groups (with each amide having two hydrogen sites: one donor and one acceptor) in dendritic peptides offers additional opportunity of formation of many intermolecular H-bonding interactions in the self-assembled gel state and hence these are amenable to supramolecular cross-linking.

Gelation properties of dendritic peptides were tested in a wide range of organic solvents using an inverted test tube method[29] (Table 1). In this typical experiment, each of the peptide gelators placed in suitable solvents was heated until it dissolved. The solution was then allowed to cool under ambient condition, and the whole volume was gelified as tested from the test tube inversion method. The organogel is very stable at room temperature. The gel melting temperature (T_{gel}) values were measured by heating the gel in an oil bath at a heating rate of 1 °C/5 min until it flows and gel melting temperatures were plotted against the concentration of the gelator peptides (Figure 2). From this figure, it has also been observed that T_{gel} increases at first sharply and then slowly as the concentration of the

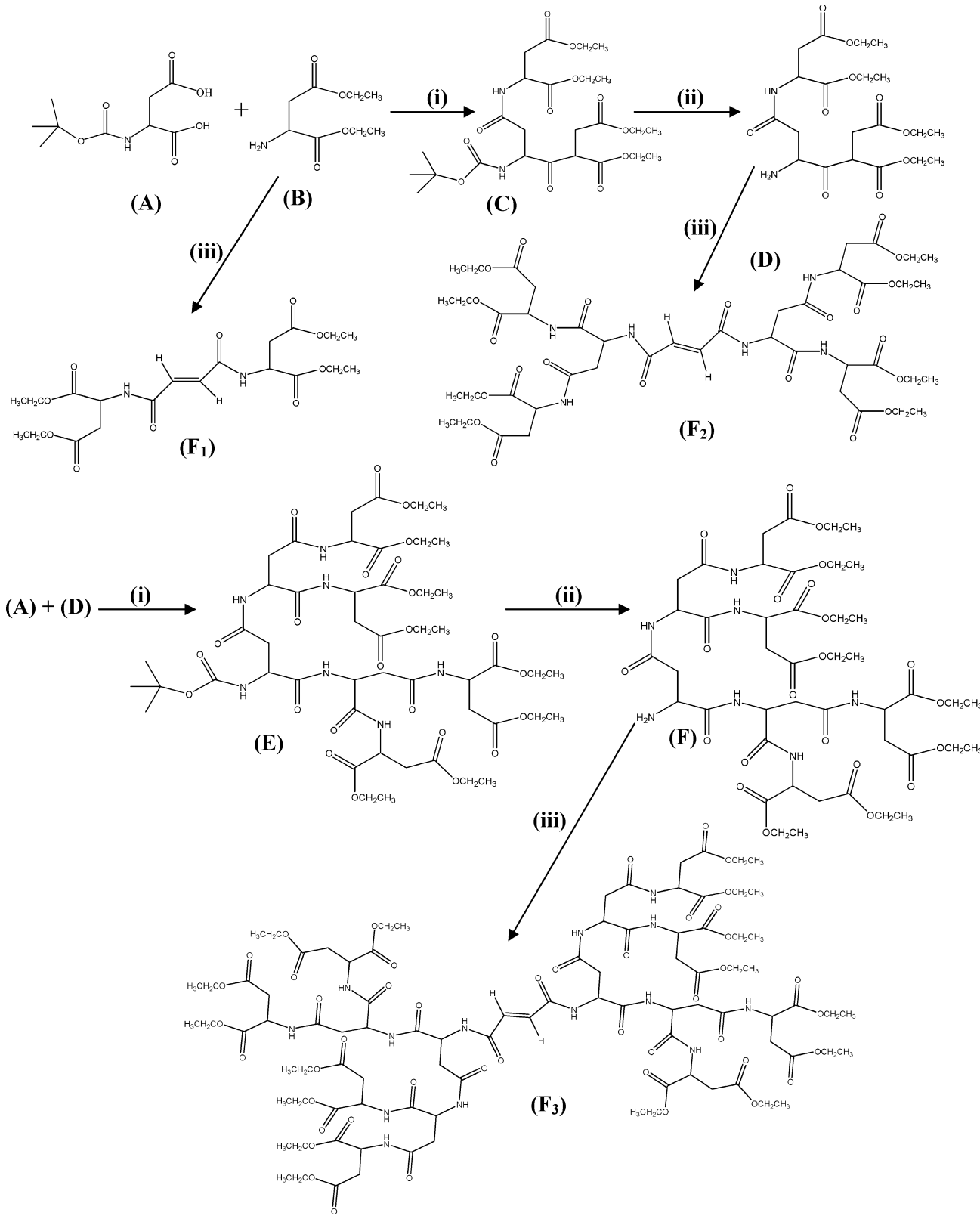

Figure 1. Schematic presentation of convergent synthesis of different generations of dendritic peptides ($\mathbf{F}_1$, $\mathbf{F}_2$, and $\mathbf{F}_3$). Reagents and conditions: (i) HOBt, DCC; (ii) TFA, $NaHCO_3$; (iii) fumaric acid, HOBt, DCC.

corresponding gelator peptide increases. It is important to note that in the T_{gel} vs concentration plot, $\mathbf{F}_2$ has a higher T_{gel} value than $\mathbf{F}_1$ and $\mathbf{F}_3$ dendrimers. This indicates that the gel obtained from $\mathbf{F}_2$ is more stable than that obtained from $\mathbf{F}_1$ and $\mathbf{F}_3$, and this is probably due to the strongest supramolecular assembly present in the system. In $\mathbf{F}_3$ one would expect better intermolecular interactions than that of the other dendritic gelators ($\mathbf{F}_1$ and $\mathbf{F}_2$). However, the lowest T_{gel} value for $\mathbf{F}_3$ gels indicates a minimum interaction in the gel state, which may be possible due to squeezing of the structure in $\mathbf{F}_3$.

Morphology. The FE-SEM images of these xerogels obtained from the corresponding dendrimers ($\mathbf{F}_1$, $\mathbf{F}_2$, and $\mathbf{F}_3$) in 1,2-dichlorobenzene reveals the fibrous morphology in their respective self-assembled state. From SEM images (Figure 3) it is

TABLE 1: Gel Forming Behavior of Three Different Dendritic Gels Obtained from Three Different Generations of Dendrimers (F_1, F_2, and F_3) in Various Organic Solvents

solvents	$\mathbf{F}_1$ (MGC)	$\mathbf{F}_2$ (MGC)	$\mathbf{F}_3$ (MGC)
1,2-dichlorobenzene	G (1.4)	G (0.63)	G (3.3)
chlorobenzene	G (2.5)	G (0.83)	G (3.3)
o-xylene	G (1.1)	G (0.70)	G (3.8)
m-xylene	G (1.0)	G (0.80)	G (4.2)
p-xylene	G (1.2)	G (0.68)	G (3.8)
tetralene	G (1.0)	G (0.83)	G (1.3)
nitrobenzene	G (2.5)	G (1.25)	G (1.25)
toluene	P	I	I
cylohexane	I	I	I
n-hexane	I	I	I
methanol	S	P	P
ethanol	S	I	I
ethylacetate	P	I	I
choloroform	S	I	I

[a] MGC: minimum gel concentration. G: gel. P: precipitation. S: soluble. I: insoluble.

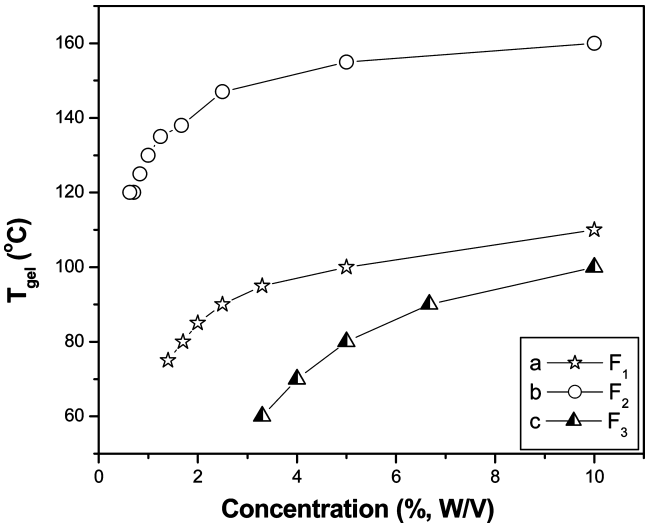

Figure 2. Change of T_{gel} with respect to gelation concentration of (a) the dendrimer $\mathbf{F}_1$ in 1,2-dichlorobenzene, (b) the dendrimer $\mathbf{F}_2$ in 1,2-dichlorobenzene, and (c) the dendrimer $\mathbf{F}_3$ in 1,2-dichlorobenzene.

observed that dendrimer $\mathbf{F}_1$ forms a tape-like morphology after self-assembly and the width of these fibers are within the range 150−200 nm. Thinner fibers have been observed for gels obtained from the second and third generation ($\mathbf{F}_2$ and $\mathbf{F}_3$) of dendritic peptides and these gel fibers are also twisted in nature, unlike the fibers obtained from the first generation of dendritic gel ($\mathbf{F}_1$). It is interesting to note that the twisted fibers are much thinner for the gels obtained from $\mathbf{F}_3$ (30−60 nm) than that of $\mathbf{F}_2$ (80−120 nm). Transmission electron microscopic images of the diluted solution of organogels obtained from dendrimers $\mathbf{F}_1$, $\mathbf{F}_2$, and $\mathbf{F}_3$ also show that dendrimers are self-aggregated to give a nanofibrillar network structure upon gelation. From the TEM observation (Figure 3), it is observed that fibrils are much thinner and these values are 70−100, 20−60, and 15−30 nm for the gels obtained from $\mathbf{F}_1$, $\mathbf{F}_2$, and $\mathbf{F}_3$ (in 1,2-dichlorobenzene) respectively. It appeared that the $\mathbf{F}_3$ system shows the dendritic type of fibrillar network. For this TEM experiment, diluted solutions of gel materials have been used. These small values of the widths of gel fibers indicate that the thinner fibrils are bundled to give wider fibrils that are observed in the FE-SEM experiments. Different widths are observed, and this is due to the fact that the procedures for preparing these samples used in these two microscopic experiments are different.[30] AFM experiments (Figure S10, Supporting Information) also give full support for the formation of the nanotape and nanofibrillar morphology in 1,2-dichlorobenzene after gel formation. These morphological variations are similar to the previous observations reported by Smith et al.[20c] using different dendritic generations. In their report, morphological changes have been observed with the variation of dendritic generations. Probably the morphology is assisted by the nature of self-assembled structure of the dendrimers; the $\mathbf{F}_1$ dendrimer has more flattened structure compared to others; hence the morphology is tape type rather than fibrils that are obtained from $\mathbf{F}_2$ and $\mathbf{F}_3$.

Thermal Behavior. The DSC experiment was carried out to scrutinize the thermoreversibility of the gel phase material. It is apparent from the DSC thermograms (Figure 4) of all three generations of these dendritic gelators that these gel phase materials show endotherms on heating and exotherms on cooling. Cooling of these gels was performed at the rate of 5 °C/min to 0 °C. It showed endotherms on further heating. The temperature difference in the endotherm and exotherm is in the range 35−65 °C and indicates hysterisis, which is a characteristic of first-order phase transition.[31] So, the fibrillar network structure and the reversible first-order phase transition clearly support the formation of thermoreversible gels by the dendritic systems.[31,32] Hence, these three dendritic peptides ($\mathbf{F}_1$, $\mathbf{F}_2$, or $\mathbf{F}_3$) produce thermoreversible organogels in 1,2-dichlorobenzene. All these samples exhibit multiple melting peaks on heating and these peaks may arise from melting of the ordered structures associated with different generations of dendrimeric chains. The melting temperature of the dendritic gels are in the order $\mathbf{F}_2 > \mathbf{F}_1 > \mathbf{F}_3$ and this order is also true for the gelation temperature (Table 2). Thus, from the DSC study, it may be concluded that $\mathbf{F}_2$ has more interacting sites than that of $\mathbf{F}_1$ and $\mathbf{F}_3$. The $\mathbf{F}_3$ is expected to have the highest number of interacting sites and the highest melting point, as $\mathbf{F}_3$ is the third generation dendrimer. However, it has been observed that it has the lowest melting point (both from visual and from DSC methods) having a minimum number of nonbonding interactions. A probable reason for that is $\mathbf{F}_3$ may have a different structure than that of $\mathbf{F}_1$ or $\mathbf{F}_2$. It would be interesting to compare the DSC melting point with the visual gel melting point. Apparent consistency between the two is found in the $\mathbf{F}_2$ and $\mathbf{F}_1$ systems: the two melting points differ by 7−8 °C. On the other hand, the $\mathbf{F}_3$ system shows a very large difference of 25 °C, and this unusual high difference in T_{gel} data may be attributed to the inherent strain present in the gel due to squeezing of the dendritic arms and when they started to flatten the gel breaks. However, the microgel system may still exist, showing a very broad DSC peak observed near 103 °C.

FT-IR Spectroscopic Study. An FT-IR study was carried out to understand the intermolecular interaction between gelator molecules in their respective gel states in 1,2-dichlorobenzene. This experiment was carried out both in the gel state and in the dilute solution state (Figure S11−S16, Supporting Information). In a very dilute solution (1 mg/mL), characteristic N−H stretching vibrations are observed at 3495.6, 3495.7, and 3495.7 cm^{-1} for dendrimers $\mathbf{F}_1$, $\mathbf{F}_2$, and $\mathbf{F}_3$, respectively. These peak values are found to be 3323.1, 3321.2, and 3288.4 cm^{-1} for the three respective peptides in their wet gel states. Similarly, if we compare the >C═O stretching bands obtained from both the dilute solution and gel state, it is observed that characteristic bands are shifted from 1692.6 to 1631.7 cm^{-1} for dendrimer $\mathbf{F}_1$, 1692.6 to 1631.7 cm^{-1} for dendrimer $\mathbf{F}_2$, and 1692.5 to 1647.1 cm^{-1} for dendrimer $\mathbf{F}_3$. The blue shift in the N−H stretching (amide A) and >C═O stretching (amide I) indicates

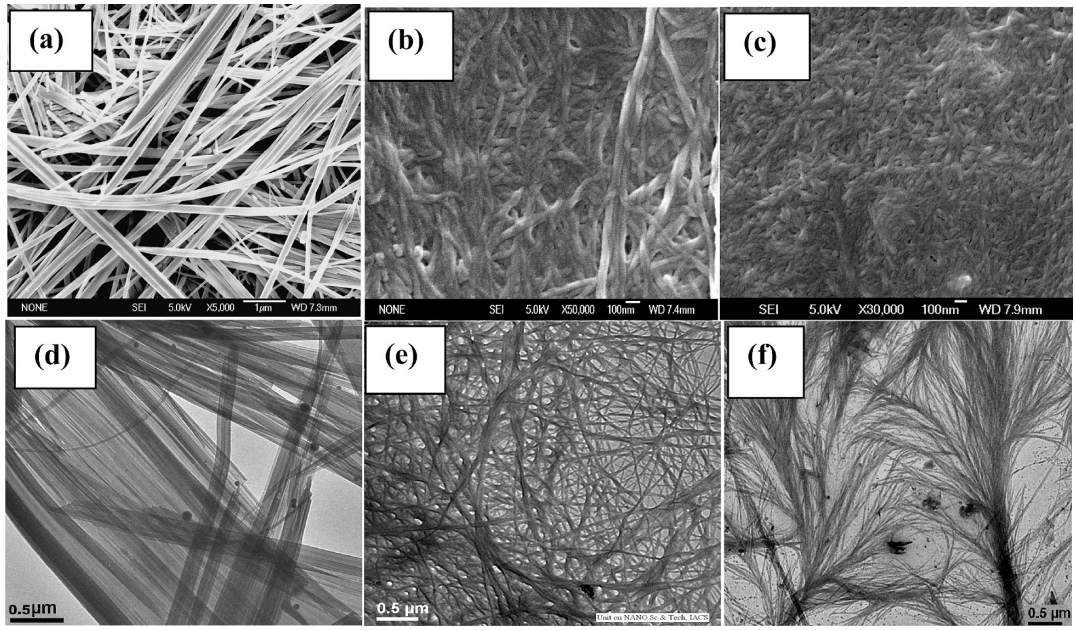

Figure 3. Field emission scanning electron microscopic (FE-SEM) images of the dendritic gels (3.5%, w/v) obtained from different generations of dendritic peptides: (a) $\mathbf{F}_1$, (b) $\mathbf{F}_2$, and (c) $\mathbf{F}_3$. High-resolution transmission electron microscopic (HR-TEM) images of the dendritic gels obtained from different generation of dendritic peptides: (d) $\mathbf{F}_1$, (e) $\mathbf{F}_2$, and (f) $\mathbf{F}_3$ in 1,2-dichlorobenzene.

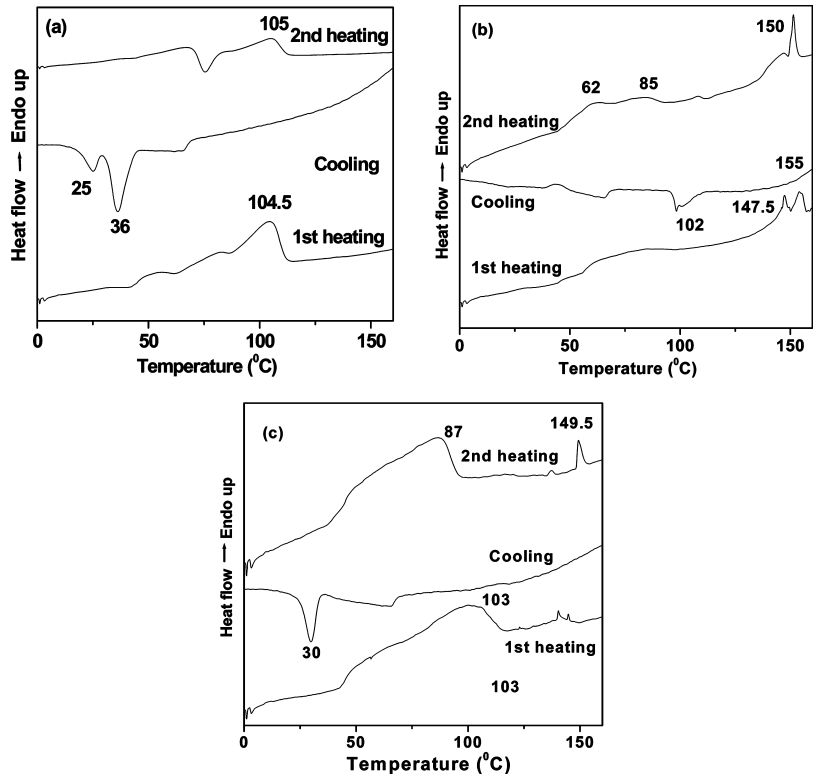

Figure 4. DSC thermograms for all three generation dendritic gelators at the same concentration (3.5, w/v %) composed of (a) organogel obtained from $\mathbf{F}_1$, (b) organogel obtained from $\mathbf{F}_2$, and (c) organogel obtained from $\mathbf{F}_3$.

the presence of hydrogen bonding in the wet gel state.[33] Moreover, we compare the >C═O stretching and NH stretching bands for all three dendrimers ($\mathbf{F}_1$, $\mathbf{F}_2$, and $\mathbf{F}_3$) in there respective gel states. It has been observed that N−H stretching frequency has been remarkably blue-shifted for $\mathbf{F}_3$ compare to that of $\mathbf{F}_1$ and $\mathbf{F}_2$. This indicates that the self-assembled structure of $\mathbf{F}_3$ dendrimer in gel state is different from that of $\mathbf{F}_1$ and $\mathbf{F}_2$.

Rheological Measurements. ***Shear Viscosity.*** The log−log plots of shear viscosity vs shear rate for three different dendritic gelators at 30 °C are shown in Figure 5. At both lower and

TABLE 2: Glass Transition Temperature, Melting Peak, and Crystallization Peak for the Three Different Dendritic Gelators ($\mathbf{F}_1$, $\mathbf{F}_2$, and $\mathbf{F}_3$) Measured from DSC Thermograms

sample	melting peak (°C) from 1st heating	crystallization peak (°C) from cooling	melting peak (°C) from 2nd heating
F_1	104.5	25, 36	105
F_2	147.5 and 155	102	62, 85, and 151
F_3	103	30	87 and 150

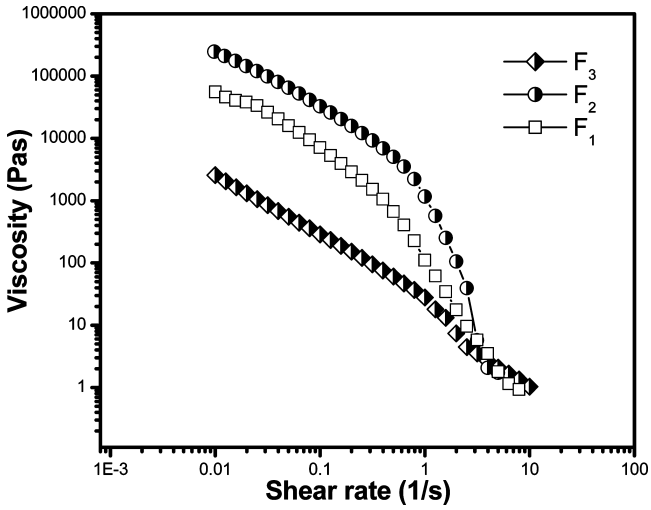

Figure 5. Steady shear viscosity vs shear rate for all three dendritic gelators obtained from different generations of dendrimers at 30 °C.

TABLE 3: Value of Zero Shear Viscosity (η_0), Characteristic Time (λ), and Power Law Exponent (n) for Three Different Dendritic Gelators (F_1, F_2, and F_3) at 30 °C

sample names	η_0 (Pa s)	λ (s)	n
F_1	33774	27	0.87
F_2	188050	5.6	0.96
F_3	1933	8.7	0.57

higher shear rates, shear viscosity increases considerably from first generation ($\mathbf{F}_1$) to second generation ($\mathbf{F}_2$) and the third generation ($\mathbf{F}_3$) has the lowest shear viscosity among them. All samples exhibit shear-thinning behavior.[31,34] To understand the flow behavior, the curves are fitted with the Carreau model $\eta = \eta_0[1 + (\lambda\dot{\gamma})]^{n-1}$, where η_0 is the zero shear viscosity, λ is the characteristic relaxation time describing the onset point of shear thinning, and n is the power law index. In Table 3, η_0, λ, and n values are presented for three different dendritic gelators. The η_0 and n values decrease from first generation to third generation, showing a maximum in second generation, but the λ value decreases from first generation to third generation showing a minimum in the second generation. Here it is to be noted that fibril-like morphology has greater zero shear viscosity than that of tape-like and/or dendritic morphology. Fibrils are three-dimensional in character, whereas the tape/dendrite has quasi two-dimensional morphology. Probably, due to the higher

TABLE 4: Exponential Values from log−log Plots of Storage and Loss Modulus versus Angular Frequency of the Dendritic Gel for Both F_1 and F_2 Systems Listed at Different Temperatures

gelator peptide	temperature (°C)	G' slope	G'' slope
$\mathbf{F}_1$	30	0.21	0.04
	50	0.4	0.14
	80	0.34	0.18
	110	1.03 (up to 10 rad/s)	0.7 (up to 10 rad/s)
		1.18 (up to 5 rad/s)	0.85 (up to 5 rad/s)
$\mathbf{F}_2$	30	0.02	0.004
	50	0.23	0.08
	80	0.38	0.09
	110	0.48 (up to 10 rad/s)	0.31 (up to 10 rad/s)
		0.62 (up to 5 rad/s)	0.41 (up to 5 rad/s)

dimensional morphology, $\mathbf{F}_2$ shows higher zero shear viscosity, as it needs a higher dragging force to flow. From the shear thinning values it may be concluded that the processing of dendritic gelators is easier in $\mathbf{F}_3$ than for $\mathbf{F}_1$ and $\mathbf{F}_2$ gels. With increasing shear rate the dendritic gelator may align to the flow direction and this may cause shear thinning of the dendritic gelators. The cause of different shear thinning in the dendritic gelator may be due to the different morphology of the dendrimers. The lower dimensional network like morphology (tape or dendrite) easily orients parallel to the flow direction than that of fibrillar morphology under shear. The tape-like morphology ($\mathbf{F}_1$), due to its higher thickness, requires a higher dragging force to be oriented parallel to the flow direction causing higher viscosity than that of $\mathbf{F}_3$.

Modulus vs Frequency. In Figure 6 the dynamic mechanical properties (e.g., storage modulus G' and loss modulus G'') of the dendritic gels are plotted with angular frequency at different temperatures. Theoretically, if $G'(\omega)$ is proportional to ω^0, $G''(\omega)$ is proportional to ω^0 and, $G'(\omega) > G''(\omega)$ (at low frequency region), the system is considered to behave as a gel. Exponential values for both $\mathbf{F}_1$ and $\mathbf{F}_2$ systems are listed in the Table 4. From this table, it is evident that the exponent values for the $\mathbf{F}_1$ and $\mathbf{F}_2$ system at 30, 50, and 80 °C are vary close to zero. So, they may be considered to behave as gels at these temperatures, while at 110 °C the slope values are really large and cannot be considered as a gel. So, it can be concluded that $\mathbf{F}_1$ and $\mathbf{F}_2$ produce gels in 1,2-dichlorobenzene up to 80 °C and at 110 °C they ($\mathbf{F}_1$ and $\mathbf{F}_2$) produce sol. It is to be noted from Figure 6a that the G' values at 50 and 80 °C are higher than that of 30 °C at all frequencies in the frequency range 0.1−100

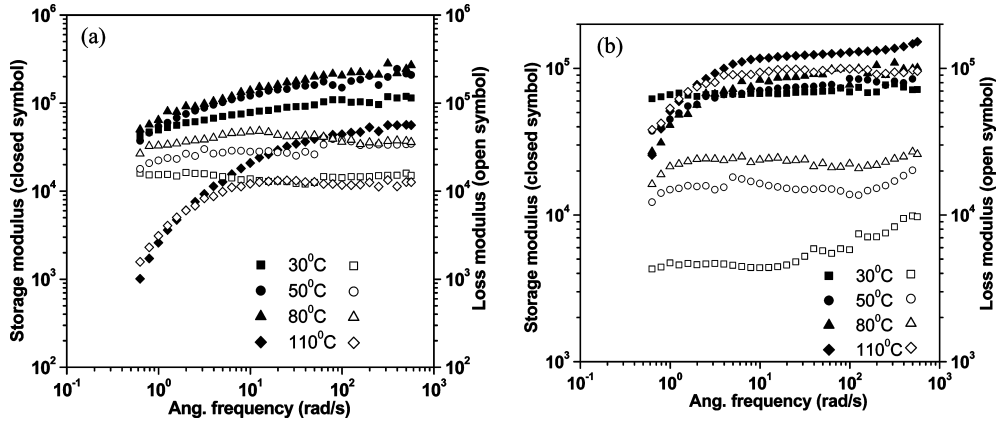

Figure 6. Log−log plots of storage (closed symbols) and loss modulus (open symbols) versus the angular frequency of the dendritic gel (3.5%, w/v) obtained from (a) the first generation of dendrimer ($\mathbf{F}_1$) and (b) the second generation of dendrimer ($\mathbf{F}_2$) at different temperatures (different symbol are indicates different temperatures).

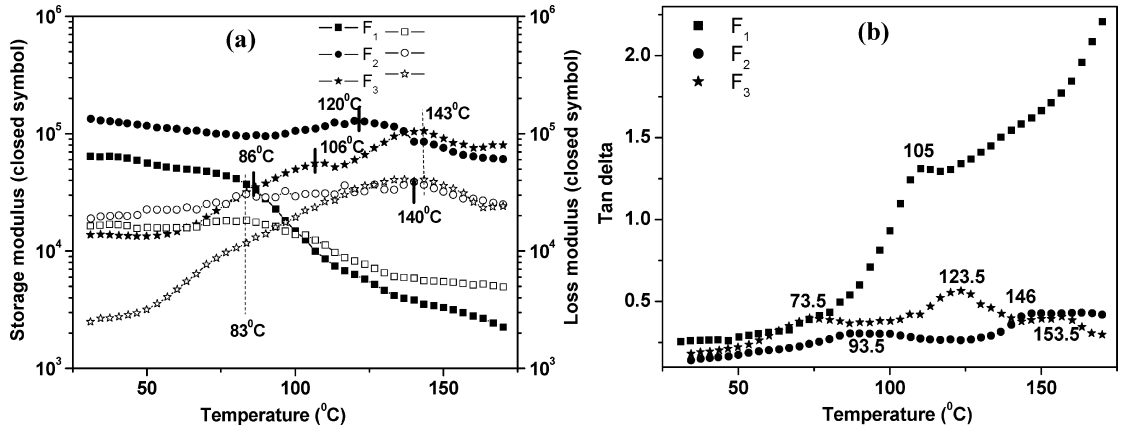

Figure 7. (a) Oscillatory viscoelastic temperature ramp curve of all the three different generations of dendrimer gels (3.5%, w/v) at a constant frequency of 1 Hz: (solid symbol = storage modulus and open symbol = loss modulus). (b) Oscillatory viscoelastic temperature ramp curve (tan δ) of all three generations of dendrimers gels (3.5%, w/v) at a constant frequency of 1 Hz.

Hz. One probable reason is that there are numerous hydrogen bonds coming from the inter/intramolecular peptide linkages and this hydrogen bonding breaks with the increase of temperature, making the dendrimers expanded, which makes the network more stronger. This results in an increase in storage modulus with temperature, except at the vicinity of the gel melting temperature (110 °C) where the network breaks. At 110 °C in the lower frequency region (<3 rad/s) the G'' are higher than G', indicating sol-like character, but with increasing frequency (>3 rad/s) the G' crossed the G'' values, indicating the system again shows gel-like (pseudosolid) behavior at higher frequency.[34,35] The same observation (Figure 6b) is true for the $\mathbf{F}_2$ dendrimer, but one important difference between $\mathbf{F}_1$ and $\mathbf{F}_2$ gels is that at 110 °C in $\mathbf{F}_2$ both G' and G'' are much higher than those at 30, 50, and 80 °C as the gel does not melt at that temperature.

Modulus vs Temperature. Figure 7a represents the oscillatory viscoelastic temperature ramp curve of all three-generation dendritic gelators at a constant frequency of 1 Hz. Here, the variation of both storage modulus and loss modulus with temperature are presented. For $\mathbf{F}_1$ with increasing temperature storage modulus gradually decreases showing a sharp fall at ~86 °C, but for $\mathbf{F}_2$ there is one maximum at ~120 °C. For $\mathbf{F}_3$ there are two maxima at ~106 and 143 °C. These transitions are well observed in loss modulus data, and the loss modulus plot shows a peak at 83 °C for $\mathbf{F}_1$, at 83 and 140 °C for $\mathbf{F}_2$, and at 84 and 143 °C for $\mathbf{F}_3$. The peak at 83 °C might be analogous to the γ transition temperature of polymers, arising from the onset of motion of the terminal group (the third segment). The transition temperature around 140 °C may be analogous to T_β showing the onset of segmental motion for the second segment. From Figure 7b, it is observed that a similar type of tan δ transitions (e.g., 105 °C for $\mathbf{F}_1$, 93.5 and 146 °C for $\mathbf{F}_2$, and 73.5 °C, 123.5 and 153.5 °C for $\mathbf{F}_3$) occurs for all three dendritic gels. The transition temperatures are different from those obtained from the loss modulus data. This is because of different mode of measurement; the loss modulus deals with the dissipation of energy while tan δ deals with damping characteristic of the samples. However, it is to be noted that in the tan δ plot for $\mathbf{F}_3$ gels we obtained three transition temperatures 73.5, 123.5, and 153.5 °C, the last one was not observed in the loss modulus data. Probably at 153.5 °C all the segmental motion starts (analogous to T_g of polymer). So, the number of transitions may be related to the molecular motion of the segments of the arms in the dendritic gelators.

Also from Figure 7a it is apparent that, for $\mathbf{F}_1$ below 100 °C the storage modulus is greater than loss modulus and above it the loss modulus is greater than that of the storage modulus. It certainly indicates that at 100 °C the gel completely melts and it is also evident from the DSC measurement. For $\mathbf{F}_2$ and $\mathbf{F}_3$ there is no crossover point, which apparently indicates that these do not melt to produce sol. However, there are two peaks at 93.5 and 146 °C for $\mathbf{F}_2$ and 73.5, 123.5, and 153.5 °C for $\mathbf{F}_3$ in tan δ. This means that at the indicated temperature there are transitions that enlarge the molecular size, yielding a higher G' value than that of G'' values. The visual gel melting occurs; however, the storage modulus increases with temperature due to elongation of the effective molecular length by the straightening of the branches. Further, from Figure 7a it is apparent that below 80 °C, the storage modulus increases from $\mathbf{F}_1$ to $\mathbf{F}_2$ and then decreases for the $\mathbf{F}_3$ dendrimer. This is possible if $\mathbf{F}_3$ has a structure different from that of $\mathbf{F}_2$. It therefore supports a view that $\mathbf{F}_3$ has a squeezed structure. Similar lowering of G' with an increase of dendrimer generation is recently reported by Chen et al.[25] So, the negative dendritic effect on storage modulus might be a general phenomena arising from the squeezing of a structure.

Conclusions

Each dendritic peptide self-assembles to form organogels in various organic solvents under suitable conditions. These gels are thermoreversible and show a first-order phase transition, as is evident from the DSC thermogramms. Morphological studies using FE-SEM, TEM, and AFM exhibit a nanofibrillar network structure that is responsible for gelation. However, FE-SEM images indicate that gel fibers obtained from first generation dendritic peptides are relatively wider than those obtained from second and/or third generation of dendritic peptides. Twisted fibers are obtained from the second and third generation of dendritic gels, while straight fibers are obtained from the first generation of a dendrtic gel. Interestingly, rheological properties of these gels vary from one generation dendrimer to other generation dendrimers. $\mathbf{F}_1$ shows regular melting of gels, i.e., the storage modulus crosses the loss modulus at 100 °C, whether $\mathbf{F}_2$ and $\mathbf{F}_3$ gels exhibit different types of properties. The storage modulus of the gel obtained from the $\mathbf{F}_2$ or $\mathbf{F}_3$ dendrimer increases with the increase of temperature. This holds the future promise of modulating the gelation behavior and their mechanical property by the proper selection of peptide-based dendritic molecules with suitable branching units.

Acknowledgment. We thank Nanoscience and Technology Initiatives, DST, Government of India, New Delhi, for their partial support. J.N. wishes to acknowledge the CSIR, New Delhi, India, for financial assistance.

Supporting Information Available: Synthesis of dendrimers, ^{1}H NMR, ^{13}C NMR, and mass spectroscopy of the reported compounds, AFM images, and FT-IR spectroscopy of dendritic gels. This material is available free of charge via the Internet at http://pubs.acs.org.

References and Notes

(1) Kobayashi, S.; Hamasaki, N.; Suzuki, M.; Kimura, M.; Shirai, H.; Hanabusa, K. *J. Am. Chem. Soc.* **2002**, *124*, 6550–6551.

(2) Shumburo, A.; Biewer, M. C. *Chem. Mater.* **2002**, *14*, 3745–3750.

(3) (a) Ray, S.; Das, A. K.; Banerjee, A. *Chem. Commun.* **2006**, 2816–2818. (b) Huang, Y.; Lin, Y.; Zeng, G.; Liang, Z.; Liu, X.; Hong, X.; Zhang, G.; Tsang, S. C. *J. Mater. Chem.* **2008**, *18*, 5445–5447.

(4) (a) Sugiyasu, K.; Fujita, N.; Shinkai, S. *Angew. Chem. Int. Ed.* **2004**, *43*, 1229–1233. (b) Ajayaghosh, A.; George, S. J.; Praveen, V. K. *Angew. Chem. Int. Ed.* **2003**, *42*, 332–335. (c) Ajayaghosh, A.; Praveen, V. K.; Vijayakumar, C. *Chem. Soc. Rev.* **2008**, *37*, 109–122.

(5) (a) Bastiat, G.; Leroux, J.-C. *J. Mater. Chem.* **2009**, *19*, 3867–3877. (b) Ray, S.; Das, A. K.; Banerjee, A. *Chem. Mater.* **2007**, *19*, 1633–1639. (c) Adhikari, B.; Palui, G.; Banerjee, A. *Soft Matter* **2009**, *5*, 3452–3460.

(6) Wilder, E. A.; Wilson, K. S.; Quinn, J. B.; Skrtic, D.; Antonucci, J. M. *Chem. Mater.* **2005**, *17*, 2946–2952.

(7) Kubo, W.; Kitamura, T.; Hanabusa, K.; Wada, Y.; Yanagida, S. *Chem. Commun.* **2002**, 374–375.

(8) (a) Jung, J. H.; Kobayashi, H.; van Bommel, K. J. C.; Shinkai, S.; Shimizu, T. *Chem. Mater.* **2002**, *14*, 1445–1447. (b) Xue, P.; Lu, R.; Huang, Y.; Jin, M.; Tan, C.; Bao, C.; Wang, Z.; Zhao, Y. *Langmuir* **2004**, *20*, 6470–6475. (c) van Esch, J. H.; Feringa, B. L. *Angew. Chem., Int. Ed.* **2000**, *39*, 2263–2266. (d) Kanie, K.; Sugimoto, T. *Chem. Commun.* **2004**, 1584–1585. (e) Love, C. S.; Chechik, V.; Smith, D. K.; Wilson, K.; Ashworth, I.; Brennan, C. *Chem. Commun.* **2005**, 1971–1973. (f) Palui, G.; Nanda, J.; Ray, S.; Banerjee, A. *Chem.—Eur. J.* **2009**, *15*, 6902–6909.

(9) (a) Terech, P.; Weiss, R. G. *Chem. Rev.* **1997**, *97*, 3133–3159. (b) Gronwald, O.; Snip, E.; Shinkai, S. *Curr. Opin. Colloid Interface Sci.* **2002**, *7*, 148–156. (c) Estroff, L. A.; Hamilton, A. D. *Chem. Rev.* **2004**, *104*, 1201–1217. (d) Abdallah, D. J.; Weiss, R. G. *Adv. Mater.* **2000**, *12*, 1237–1247. (e) Shimizu, T. *Polym. J.* **2003**, *35*, 1–22. (f) Sangeetha, N. M.; Maitra, U. *Chem. Soc. Rev.* **2005**, *34*, 821–836. (g) Suzuki, M.; Hanabusa, K. *Chem. Soc. Rev.* **2009**, *38*, 967–975. (h) Banerjee, S.; Das, R. K.; Maitra, U. *J. Mater. Chem.* **2009**, *19*, 6649–6687. (i) Wu, J.; Tian, Q.; Hu, H.; Xia, Q.; Zou, Y.; Li, F.; Yi, T.; Huang, C. *Chem. Commun.* **2009**, 4100–4102. (j) Gasnier, A.; Royal, G.; Terech, P. *Langmuir* **2009**, *25*, 8751–8762. (k) Terech, P.; Maitra, U. *J. Phys. Chem. B* **2008**, *112*, 13483–13492.

(10) (a) Suzuki, M.; Yumoto, M.; Shirai, H.; Hanabusa, K. *Chem.—Eur. J.* **2008**, *14*, 2133–2144. (b) Hanabusa, K.; Tanaka, R.; Suzuki, M.; Kimura, M.; Shirai, H. *Adv. Mater.* **1997**, *9*, 1095–1097. (c) Bhattacharya, S.; Srivastava, A.; Pal, A. *Angew. Chem., Int. Ed.* **2006**, *45*, 2934–2937. (d) Bhattacharya, S.; Ghosh, Y. K. *Chem. Commun.* **2001**, 185–186. (e) Bhattacharya, S.; Acharya, S. N. G. *Chem. Mater.* **1999**, *11*, 3121–3132. (f) Bhattacharya, S.; Acharya, S. N. G.; Raju, A. R. *Chem. Commun.* **1996**, 2101–2102. (g) Mieden-Gundert, G.; Klein, L.; Fischer, M.; Vögtle, F.; Heuzé, K.; Pozzo, J.-L.; Vallier, M.; Fages, F. *Angew. Chem., Int. Ed.* **2001**, *40*, 3164–3166. (h) D'Aléo, A.; Pozzo, J.-L.; Fages, F.; Schmutz, M.; Mieden-Gundert, G.; Vögtle, F.; Caplar, V.; Zinic, M. *Chem. Commun.* **2004**, 190–191. (i) D'Aléo, A.; Pozzo, J.-L.; Heuzé, K.; Vögtle, F.; Fages, F. *Tetrahedron* **2007**, *63*, 7482–7488.

(11) (a) Ajayaghosh, A.; Praveen, V. K. *Acc. Chem. Res.* **2007**, *40*, 644–656. (b) Guerzo, A. D.; Olive, A. G. L.; Reichwagen, J.; Hopf, H.; Desvergne, J.-P. *J. Am. Chem. Soc.* **2005**, *127*, 17984–17985. (c) Goodson, T., III; Li, W.; Gharavi, A.; Yu, L. *Adv. Mater.* **1997**, *9*, 639–643. (d) Shu, T.; Wu, J.; Lu, M.; Chen, L.; Yi, T.; Li, F.; Huang, C. *J. Mater. Chem.* **2008**, *18*, 886–893.

(12) (a) Samanta, S. K.; Pal, A.; Bhattacharya, S. *Langmuir* **2009**, *25*, 8567–8578. (b) Sugiyasu, K.; Fujita, N.; Shinkai, S. *J. Mater. Chem.* **2005**, *15*, 2747–2754. (c) Chung, J. W.; Yoon, S.-J.; Lim, S.-J.; An, B.-K.; Park, S. Y. *Angew. Chem., Int. Ed.* **2009**, *48*, 7030–7034. (d) Li, X.-Q.; Zhang, X.; Ghosh, S.; Würthner, F. *Chem.—Eur. J.* **2008**, *14*, 8074–8078. (e) Kamikawa, Y.; Kato, T. *Langmuir* **2007**, *23*, 274–278. (f) Srivastava, A.; Ghorai, S.; Bhattacharjya, A.; Bhattacharya, S. *J. Org. Chem.* **2005**, *70*, 6574–6582.

(13) Bhattacharya, S.; Samanta, S. K. *Langmuir* **2009**, *25*, 8378–8381.

(14) (a) Smith, D. K. *Adv. Mater.* **2006**, *18*, 2773–2778. (b) Newkome, G. R.; Baker, G. R.; Saunders, M. J.; Russo, P. S.; Gupta, V. K.; Yao, Z.-q.; Miller, J. E.; Bouillion, K. *J. Chem. Soc., Chem. Commun.* **1986**, 752–753. (c) Jang, W.-D.; Jiang, D.-L.; Aida, T. *J. Am. Chem. Soc.* **2000**, *122*, 3232–3233. (d) Jang, W.-D.; Aida, T. *Macromolecules* **2003**, *36*, 8461–8469. (e) Ji, Y.; Luo, Y.-F.; Jia, X.-R.; Chen, E.-Q.; Huang, Y.; Ye, C.; Wang, B.-B.; Zhou, Q.-F.; Wei, Y. *Angew. Chem., Int. Ed.* **2005**, *44*, 6025–6029. (f) Li, W.-S.; Jia, X.-R.; Wang, B.-B.; Ji, Y.; Wei, Y. *Tetrahedron* **2007**, *63*, 8794–8800. (g) Ko, H. S.; Park, C.; Lee, S. M.; Song, H. H.; Kim, C. *Chem. Mater.* **2004**, *16*, 3872–3876.

(15) (a) Newkome, G. R.; Baker, G. R.; Arai, S.; Saunders, M. J.; Russo, P. S.; Theriot, K. J.; Moorefield, C. N.; Rogers, L. E.; Miller, J. E.; Lieux, T. R.; Murray, M. E.; Phillips, B.; Pascal, L. *J. Am. Chem. Soc.* **1990**, *112*, 8458–8465. (b) Newkome, G. R.; Lin, X.; Yaxiong, C.; Escamilla, G. H. *J. Org. Chem.* **1993**, *58*, 3123–3129.

(16) Zhang, W.; Gonzalez, S. O.; Simanek, E. E. *Macromolecules* **2002**, *35*, 9015–9021.

(17) (a) Carnahan, M. A.; Middleton, C.; Kim, J.; Kim, T.; Grinstaff, M. W. *J. Am. Chem. Soc.* **2002**, *124*, 5291–5293. (b) Wathier, M.; Jung, P. J.; Carnahan, M. A.; Kim, T.; Grinstaff, M. W. *J. Am. Chem. Soc.* **2004**, *126*, 12744–12745.

(18) (a) Zubarev, E. R.; Stupp, S. I. *J. Am. Chem. Soc.* **2002**, *124*, 5762–5773. (b) de Gans, B. J.; Wiegand, S.; Zubarev, E. R.; Stupp, S. I. *J. Phys. Chem. B* **2002**, *106*, 9730–9736.

(19) (a) Huang, B.; Hirst, A. R.; Smith, D. K.; Castelletto, V.; Hamley, I. W. *J. Am. Chem. Soc.* **2005**, *127*, 7130–7139. (b) Duan, P.; Liu, M. *Langmuir* **2009**, *25*, 8706–8713.

(20) (a) Partridge, K. S.; Smith, D. K.; Dykes, G. M.; McGrail, P. T. *Chem. Commun.* **2001**, 319–320. (b) Hirst, A. R.; Smith, D. K.; Feiters, M. C.; Geurts, H. P. M.; Wright, A. C. *J. Am. Chem. Soc.* **2003**, *125*, 9010–9011. (c) Love, C. S.; Hirst, A. R.; Chechik, V.; Smith, D. K.; Ashworth, I.; Brennan, C. *Langmuir* **2004**, *20*, 6580–6585. (d) Hirst, A. R.; Smith, D. K.; Feiters, M. C.; Geurts, H. P. M. *Langmuir* **2004**, *20*, 7070–7077. (e) Hirst, A. R.; Smith, D. K.; Feiters, M. C.; Geurts, H. P. M. *Chem.—Eur. J.* **2004**, *10*, 5901–5910. (f) Smith, D. K. *Chem. Commun.* **2006**, 34–44.

(21) (a) Kim, C.; Kim, K. T.; Chang, Y.; Song, H. H.; Cho, T.-Y.; Jeon, H.-J. *J. Am. Chem. Soc.* **2001**, *123*, 5586–5587. (b) Kim, C.; Lee, S. J.; Lee, I. H.; Kim, K. T.; Song, H. H.; Jeon, H.-J. *Chem. Mater.* **2003**, *15*, 3638–3642.

(22) Kuang, G.-C.; Ji, Y.; Jia, X.-R.; Li, Y.; Chen, E.-Q.; Wei, Y. *Chem. Mater.* **2008**, *20*, 4173–4175.

(23) Ji, Y.; Kuang, G.-C.; Jia, X.-R.; Chen, E.-Q.; Wang, B.-B.; Li, W.-S.; Wei, Y.; Lei, J. *Chem. Commun.* **2007**, 4233–4235.

(24) Chow, H.-F.; Zhang, J. *Chem.—Eur. J.* **2005**, *11*, 5817–5831.

(25) Chen, Y.; Lv, Y.; Han, Y.; Zhu, B.; Zhang, F.; Bo, Z.; Liu, C.-Y. *Langmuir* **2009**, *25*, 8548–8555.

(26) (a) Maji, S. K.; Malik, S.; Drew, M. G. B.; Nandi, A. K.; Banerjee, A. *Tetrahedron Lett.* **2003**, *44*, 4103–4107. (b) Malik, S.; Maji, S. K.; Banerjee, A.; Nandi, A. K. *J. Chem. Soc., Perkin Trans. 2* **2002**, 1177–1186. (c) Das, A. K.; Manna, S.; Drew, M. G. B.; Malik, S.; Nandi, A. K.; Banerjee, A. *Supramol. Chem.* **2006**, *18*, 645–655. (d) Das, A. K.; Bose, P. P.; Drew, M. G. B.; Banerjee, A. *Tetrahedron* **2007**, *63*, 7432–7442. (e) Banerjee, A.; Palui, G.; Banerjee, A. *Soft Matter* **2008**, *4*, 1430–1437.

(27) Palui, G.; Simon, F.-X.; Schmutz, M.; Mesini, P. J.; Banerjee, A. *Tetrahedron* **2008**, *64*, 175–185.

(28) (a) Ragunathan, K. G.; Bhattacharya, S. *Chem. Phys. Lipids.* **1995**, *77*, 13–23. (b) Pal, A.; Ghosh, Y. K.; Bhattacharya, S. *Tetrahedron* **2007**, *63*, 7334–7348.

(29) Murata, K.; Aoki, M.; Suzuki, T.; Harada, T.; Kawabata, H.; Komori, T.; Ohseto, F.; Ueda, K.; Shinkai, S. *J. Am. Chem. Soc.* **1994**, *116*, 6664–6676.

(30) Malik, S.; Kawano, S.-i.; Fujita, N.; Shinkai, S. *Tetrahedron* **2007**, *63*, 7326–7333.

(31) (a) Dasgupta, D.; Manna, S.; Garai, A.; Dawn, A.; Rochas, C.; Guenet, J. M.; Nandi, A. K. *Macromolecules* **2008**, *41*, 779–787. (b) Garai, A.; Nandi, A. K. *J. Polym. Sci., Part B: Polym. Phys.* **2008**, *46*, 28–40.

(32) Daniel, C.; Dammer, C.; Guenet, J.-M. *Polymer* **1994**, *35*, 4243–4246.

(33) Palui, G.; Banerjee, A. *J. Phys. Chem. B* **2008**, *112*, 10107–10115.

(34) Uppuluri, S.; Keinath, S. E.; Tomalia, D. A.; Dvornic, P. R. *Macromolecules* **1998**, *31*, 4498–4510.

(35) (a) Lorén, N.; Shtykova, L.; Kidman, S.; Jarvoll, P.; Nydén, M.; Hermansson, A.-M. *Biomacromolecules* **2009**, *10*, 275–284. (b) Tande, B. M.; Wagner, N. J.; Kim, Y. H. *Macromolecules* **2003**, *36*, 4619–4623.

JP908011V